Intersubband optical absorption coefficients and refractive index changes in spherical hydrogenic antidots

© S. Davatolhagh¶, R. Khordad*, A.R. Jafari+

Department of Physics, College of Sciences, Shiraz University, Shiraz, 71454 Iran
* Department of Physics, College of Sciences, Yasouj University, Yasouj, 75914-353 Iran
+ Department of Physics, Lamerd Branch, Islamic Azad University, Lamerd, Iran

(Получена 14 октября 2012 г. Принята к печати 13 июня 2013 г.)

In this work, we have studied the optical absorption coefficients and refractive index changes in spherical quantum antidots with hydrogenic donor impurity at the center. For this purpose, the energy spectrum and wavefunctions are first determined, analytically. Then, we have used analytical expressions for the intersubband absorption coefficients and refractive index changes obtained by the compact density matrix formalism. The results show that i) total absorption coeficient increase with increasing size of antidot, ii) the refractive index changes decrease with decreasing antidot size.

1. Introduction

In the past few years, low-dimensional semiconductor systems have been received considerable attention due to their fundamental properties and their wide range of applications [1–3]. One of the most intensively explored classes of the systems is the class of quantum antidots. Modern microfabrication technology has allowed scientists to fabricate quantum antidots. Quantum confinement of charge carriers in quantum antidots leads to formation of discrete energy levels and the change of electronic and optical properties [4–6].

Recent advances in the fabrication of semiconductor nanostructures like molecular beam epitaxy and metal organic vapor-phase epitaxy makes it possible to construct semiconductor nano-scale objects with a wide range of geometries. Among the semiconductor nano-scale structures, a great attention has been devoted to the physics of the semiconductor quantum antidots (QAD) mainly due to their applications in optics and optoelectronics [7–9].

QADs confine charge carriers in two or three dimensions and their size, shape, and other properties can be controlled in experiments. This attractiveness, the controlling physical properties of a QAD, is not only from the fundamental scientific point of view, but also for its potential application in the development of semiconductor optoelectronics devices. In recent years, the electronic properties of QADs have been widely studied [10,11].

Hitherto, some works have been made about electronic properties of QADs [10–13]. In the present work, we intend to study the optical properties of a medium with an ensemble of antidots. We first solve analytically the Schrödinger equation to obtain the energy levels and wavefunctions. Using the obtained energy levels and wavefunctions, we calculate the optical properties of spherical hedrogenic QADs. The purpose of the present work is to obtain the changes in the linear and third order non-linear refractive index we well as absorption coefficient for the $GaAs/Al_xGa_{1-x}As$ medium in the presence of hydrogenic antidot, using the density matrix formalism. It is to be noted that the antidots are single charged by electrons.

The paper is organized as follows: In Sec. 2, an QAD is described. Then, the electron energy levels and wave functions are presented analytically. In Sec. 3, analytical expressions for the total intersubband optical absorption coeficients and refractive index changes are obtained using the density matrix approach. The results and discussion are presented in Sec. 4 and finally, the conclusion is summarized in Sec. 5.

2. Theory and model

In this part, we intend to study the energy levels of semiconductor quantum antidots within the effective mass approximation. The Hamiltonian a single electron in a quantum antidots can be written as

$$H = -\frac{\hbar^2}{2m^*}\nabla^2 + V(r), \tag{1}$$

where m^* is the electron effective mass and $V(r)$ represents a confinement potential. This potential energy function of the hydrogenic quantum antidots is given by

$$V(r) = \begin{cases} V_0 - \frac{e^2}{\varepsilon r}, & r < r_0 \\ -\frac{e^2}{\varepsilon r}, & r > r_0, \end{cases} \tag{2}$$

where r_0 is the antidot's radius, ε is the dielectric constant of the medium, and V_0 is the height of the potential energy barrier. It is to be noted that the potential energy barrier V_0, arises due to a mismatch between the electronic affinities of the two regions.

To find wavefunctions and energy levels of the Hamiltonian (1), we must solve the Schrödinger equation using

¶ E-mail: khordad@mail.yu.ac.ir

separable method, $\psi(r,\theta,\varphi) = R(r)Y(\theta,\varphi)$. With respect to Eqs (1) and (2), the Schrödinger equation can be reduced to the radial equation which depends on only one coordinate.

Since the potential (2) is spherically symmetric, we are going to use the spherical coordinates. In the spherical coordinates, the radial part of the Schrödinger equation in the two regions, is given by

$$-\frac{\hbar^2}{2m^*}\left[\frac{1}{r}\frac{d}{dr}\left(r\frac{d}{dr}\right)+\frac{1}{r}\frac{d}{dr}-\frac{l(l+1)}{r^2}\right]R_1(r) + \left(E - V_0 + \frac{e^2}{\varepsilon r}\right)R_1(r) = 0, \quad r < r_0, \quad (3)$$

and

$$-\frac{\hbar^2}{2m^*}\left[\frac{1}{r}\frac{d}{dr}\left(r\frac{d}{dr}\right)+\frac{1}{r}\frac{d}{dr}-\frac{l(l+1)}{r^2}\right]R_2(r) + \left(E + \frac{e^2}{\varepsilon r}\right)R_2(r) = 0, \quad r > r_0. \quad (4)$$

The solutions of above equation yield the allowed energy eigenvalues E and the corresponding wave functions $R(r)$. To solve Eqs (3) and (4), we use the following definitions:

$$\alpha_1^2 = -\frac{8m^*(E - V_0)}{\hbar^2}, \quad \alpha_2^2 = -\frac{8m^*(E)}{\hbar^2},$$

$$\lambda_1 = \frac{2m^*e^2}{\varepsilon\hbar^2\alpha_1^2}, \quad \lambda_2 = \frac{2m^*e^2}{\varepsilon\hbar^2\alpha_2^2}. \quad (5)$$

Also, we apply the following change of variables

$$\rho_1 = \alpha_1 r, \quad \rho_2 = \alpha_2 r. \quad (6)$$

Now, using the definition $R_i(\rho) = \frac{1}{\rho}G_i(\rho)$ $(i = 1, 2)$, the Schrödinger equations (3) and (4) convert to the following equations [13]:

$$\frac{d^2G_1(\rho_1)}{d\rho_1^2} + \left(-\frac{1}{4} + \frac{\lambda_1}{\rho_1} + \frac{\frac{1}{4} - (l+\frac{1}{2})^2}{\rho_1^2}\right)G_1(\rho_1) = 0, \quad r < r_0, \quad (7)$$

$$\frac{d^2G_2(\rho_2)}{d\rho_2^2} + \left(-\frac{1}{4} + \frac{\lambda_2}{\rho_2} + \frac{\frac{1}{4} - (l+\frac{1}{2})^2}{\rho_2^2}\right)G_2(\rho_2) = 0, \quad r > r_0. \quad (8)$$

It is worth mentioning that these equations are the Whittaker equations [4]. Now we can write the most general solutions in terms of the Whittaker functions as below

$$G_1(\rho_1) = A_1U_1\left(\lambda_1, l+\frac{1}{2};\rho_1\right) + B_1W_1\left(\lambda_1, l+\frac{1}{2};\rho_1\right), \quad r < r_0, \quad (9)$$

$$G_2(\rho_2) = A_2U_2\left(\lambda_2, l+\frac{1}{2};\rho_2\right) + B_2W_2\left(\lambda_2, l+\frac{1}{2};\rho_2\right), \quad r > r_0 \quad (10)$$

where U_i and W_i are the Whittaker functions. Also, A_i and B_i are normalication constants which must be determine by the continuity and the asymptotic conditions. Considering the asymptotic behaviors of the wavefunctions, we have $A_2 = B_1 = 0$ due to the Whittaker functions W_1 and U_2 diverge at the origin and infinity, respectively. Now, using the relation $R_i(\rho) = \frac{1}{\rho}G_i(\rho)$, one can write the radial part of the wavefunctions as below

$$R_1(\rho_1) = \frac{1}{\rho_1}G_1(\rho_1) = \frac{A_1}{\rho_1}U_1\left(\lambda_1, l+\frac{1}{2};\rho_1\right), \quad r < r_0, \quad (11)$$

$$R_2(\rho_2) = \frac{1}{\rho_2}G_2(\rho_2) = \frac{B_2}{\rho_2}W_2\left(\lambda_2, l+\frac{1}{2};\rho_2\right), \quad r > r_0. \quad (12)$$

Here, we can use the relation between the Whittaker functions and the hypergeometric functions [14]. Therefore, the radial part of the wavefunctions reduces to

$$R_1(\rho_1) = A_1\rho_1^l\exp\left(-\frac{\rho_1}{2}\right)M_1(l+1-\lambda_1, 2+2l;\rho_1), \quad r < r_0, \quad (13)$$

$$R_2(\rho_2) = B_2\rho_2^l\exp\left(-\frac{\rho_2}{2}\right)M_2(l+1-\lambda_2, 2+2l;\rho_2), \quad r > r_0, \quad (14)$$

where M_1 and M_2 are the hypergeometric functions [14]. Therefore, the total wave function can be written as $\psi_{\lambda lm}(r,\theta,\varphi) = R_{\lambda l}(r)Y_{lm}(\theta,\varphi)$. There are three quantum numbers in this wave function.

3. Optical absorption coefficients and refractive index changes

In this section we used the density matrix formalism to calculate the refractive index changes and optical absorption coeficients for a quantum antidot structure, corresponding to an optical transition between two subbands. It should note that the antidots are single charged by electrons.

As we know, the system under study can be excited by an electromagnetic field of frequency ω, such as

$$E(t) = \tilde{E}e^{i\omega t} + \tilde{E}e^{-i\omega t}. \quad (15)$$

The time evolution of the matrix elements of one-electron density operator, ρ, can be written as [15,16]

$$\frac{\partial\rho}{\partial t} = \frac{1}{i\hbar}\left[H_0 - qzE(t), \rho\right] - \Gamma(\rho - \rho^{(0)}), \quad (16)$$

where H_0 is the Hamiltonian for this system without the electromagnetic field $E(t)$, q is the electronic charge. The symbol $[\sim]$ is the quantum mechanical commutator, $\rho^{(0)}$

is the unperturbed density matrix operator, and Γ is the phenomenological operator responsible for the damping due to the electron-phonon interaction, collisions among electrons, etc. This phenomenological damping term indicates that ρ relaxes to its equilibrium value $\rho^{(0)}$ at rate Γ. Since Γ is a decay rate, it is assumed that $\Gamma_{nm} = \Gamma_{mn}$. In addition, we make the physical assumption that $\rho^{(0)}_{mn} = 0$ for $m \neq n$.

It is assumed that Γ is a diagonal matrix and its elements are equal to the inverse of relaxation time T ($\Gamma_{mm} = \frac{1}{T_{mm}}$). The damping rates Γ_{mn} for the off-diagonal elements of the density matrix are not entirely independent of the damping rates of the diagonal elements. In fact, under quite general conditions the off-diagonal elements can be represented as

$$\Gamma_{mn} = \frac{1}{2}(\Gamma_{mm} + \Gamma_{nn}), \tag{17}$$

where Γ_m and Γ_n denote the total decay rates of population out levels m and n, respectively [17].

Eq. (16) can be solved using the standard iterative method by expanding ρ [18]:

$$\rho(t) = \sum_n \rho^{(n)}(t), \tag{18}$$

with

$$\frac{\partial \rho^{(n+1)}_{ij}}{\partial t} = \frac{1}{i\hbar}[H_0, \rho^{(n+1)}]_{ij} - \Gamma_{ij}\rho^{(n+1)}_{ij} - \frac{1}{i\hbar}[qx, \rho^{(n)}]_{ij}E(t). \tag{19}$$

For simplicity, we shall only confine our attention to two-level electronic systems for electronic transitions. Therefore, the electronic polarization $P(t)$ and susceptibility $\chi(t)$ are expressed by dipole operator M and density matrix ρ

$$P(t) = \varepsilon_0\chi(\omega)\tilde{E}e^{-i\omega t} + \varepsilon_0\chi(-\omega)\tilde{E}^*e^{i\omega t} = \frac{1}{V}\mathrm{Tr}(\rho M), \tag{20}$$

where ρ and V are the one-electron density matrix and the volume of the system, ε_0 is the permittivity of free space, and the symbol Tr (trace) denotes the summation over the diagonal elements of the matrix.

The analytical forms of the linear $\chi^{(1)}$ and the third-order nonlinear $\chi^{(3)}$ susceptibility coeficients are obtained from Eqs (19) and (20) as

$$\varepsilon_0\chi^{(1)}(\omega) = \frac{\sigma_v|M_{21}|^2}{E_{21} - \hbar\omega - i\hbar\Gamma_{12}}, \tag{21}$$

$$\varepsilon_0\chi^{(3)}(\omega) = -\frac{\sigma_v|M_{21}|^2|E|^2}{E_{21} - \hbar\omega - i\hbar\Gamma_{12}}\left[\frac{4|M_{21}|^2}{(E_{21} - \hbar\omega)^2 + (\hbar\Gamma_{12})^2} - \frac{(M_{22} - M_{11})^2}{(E_{21} - i\hbar\Gamma_{12})(E_{21} - \hbar\omega - i\hbar\Gamma_{12})}\right], \tag{22}$$

where σ_v is the density of antidots. The refractive index changes is related to the susceptibility as [19]

$$\frac{\Delta n(\omega)}{n_r} = \mathrm{Re}\left[\frac{\chi(\omega)}{2n_r^2}\right], \tag{23}$$

where n_r is the refractive index. By using Eqs (21)–(23), the linear and the third-order nonlinear refractive index changes can be expressed as [19]

$$\frac{\Delta n^{(1)}(\omega)}{n_r} = \frac{\sigma_v|M_{21}|^2}{2n_r^2\varepsilon_0}\left[\frac{E_{21} - \hbar\omega}{(E_{21} - \hbar\omega)^2 + (\hbar\Gamma_{12})^2}\right], \tag{24}$$

and

$$\frac{\Delta n^{(3)}(\omega)}{n_r} = -\frac{\sigma_v|M_{21}|^2}{4n_r^3\varepsilon_0}\frac{\mu c I}{[(E_{21} - \hbar\omega)^2 + (\hbar\Gamma_{12})^2]^2} \times \left[4(E_{21} - \hbar\omega)|M_{21}|^2 - \frac{(M_{22} - M_{11})^2}{(E_{21})^2 + (\hbar\Gamma_{12})^2}\Big\{(E_{21} - \hbar\omega) \times \left[E_{21}(E_{21} - \hbar\omega) - (\hbar\Gamma_{12})^2\right] - (\hbar\Gamma_{12})^2(2E_{21} - \hbar\omega)\Big\}\right], \tag{25}$$

where μ is the permeability, $E_{ij} = E_i - E_j$, and $M_{ij} = |\langle\psi_i|qz|\psi_j\rangle|$ is the electric dipole moment matrix element. Since the electromagnetic field is in the z direction, we have applied the following selection rules $\Delta l = 1$, $\Delta m = 0$ for optical transitions.

The symbol I is the optical intensity of the incident wave and expressed as

$$I = 2\sqrt{\frac{\varepsilon_R}{\mu}}|E(\omega)|^2 = \frac{2n_r}{\mu c}|E(\omega)|^2, \tag{26}$$

where c is the speed of light in free space.

The transition dipole moment or transition moment M_{ij}, usually denoted for a transition between an initial state, i, and a final state, j, is the electric dipole moment associated with the transition between the two states. In ganeral, the transition dipole moment is a complex vector quantity that includes the phase factors associated with the two states. Its direction gives the platrization of the transition, which determines how the system will interact with an electromagnetic wave of a given polarization, while the square of the magnitude gives the strength of the interaction due to the distribution of charge within the system. The *SI* unit of the transition dipole moment is the Coulomb-meter (Cm); a more conveniently sized unit is the Debye (D). The transition dipole moment for the transition is given by the relevant off-diagonal element of the diople of matrix, which can be calculated from an integral taken over the product of the wavefunctions of the initial and final states of the transition, and the dipole moment operator. On the basis of the implicit assumption that the initial and final states have definite parity, the diagonal elements of the dipole moment matrix are equal to zero (a consequence of symmetry considerations).

Using Eqs. (24) and (25), one can write the total refractive index change as

$$\frac{\Delta n(\omega)}{n_r} = \frac{\Delta n^{(1)}(\omega)}{n_r} + \frac{\Delta n^{(3)}(\omega)}{n_r}. \tag{27}$$

The susceptibility $\chi(\omega)$ is related to the absorption coefficient $\alpha(\omega)$ and real part of permittivity ε_R as:

$$\alpha(\omega) = \omega\sqrt{\frac{\mu}{\varepsilon_R}}\,\mathrm{Im}[\varepsilon_0\chi(\omega)]. \tag{28}$$

Now, the linear and third-order nonlinear absorption coefficient can be written as [14,20]

$$\alpha^{(1)}(\omega) = \omega\sqrt{\frac{\mu}{\varepsilon_R}}\left[\frac{\sigma_v \hbar\Gamma_{12}|M_{21}|^2}{(E_{21}-\hbar\omega)^2+(\hbar\Gamma_{12})^2}\right], \qquad (29)$$

$$\alpha^{(3)}(\omega, I) = -\omega\sqrt{\frac{\mu}{\varepsilon_R}}\left(\frac{I}{2\varepsilon_0 n_r c}\right)\frac{\sigma_v \hbar\Gamma_{12}|M_{21}|^2}{[(E_{21}-\hbar\omega)^2+(\hbar\Gamma_{12})^2]^2}$$

$$\times\left\{4|M_{21}|^2 - \frac{[3E_{21}^2 - 4E_{21}\hbar\omega + \hbar^2(\omega^2-\Gamma_{12}^2)]}{E_{21}^2+(\hbar\Gamma_{21})^2}\right\}. \qquad (30)$$

Using Eqs (29) and (30), one can express the total absorption coefficient $\alpha(\omega, I)$ as [14,16]

$$\alpha(\omega, I) = \alpha^{(1)}(\omega) + \alpha^{(3)}(\omega, I). \qquad (31)$$

4. Numerical results

In the following, we will discuss the total refractive index and absorption coefficient changes in GaAs/Al_xGa_{1-x}As semiconductor quantum antidots. Here, x is the Al concentration. It is worth mentioning that V_0 is related to Al concentration as

$$V_0\,[\text{eV}] = 0.6(1.04x + 0.47x^2). \qquad (32)$$

The used parameters for GaAs/Al_xGa_{1-x}As semiconductor quantum antidot are: $n_r = 3.2$, $T_{12} = 0.2$ ps, $\Gamma_{12} = 1/T_{12}$, and $\sigma_v = 3.0\cdot 10^{16}\,\text{cm}^{-3}$, $a_0 = \frac{\hbar^2\varepsilon}{m^* e^2}$, and $\text{R}_\text{y} = \frac{m^* e^4}{2\hbar^2\varepsilon^2}$.

In Fig. 1, the total refractive index changes is plotted as a function of the photon energy for five different antidot size 0.01, 1.0, 2.0, 6, and $10a_0$ with $I = 0.2\,\text{MW/cm}^2$ and $V_0 = 2\,\text{R}_\text{y}$. This figure clearly shows that the total refractive index change is related strongly to the antidot size. As the antidot size increases, the total refractive index changes increase and also shift towards lower energies. This is because the energy difference decreases when the antidot size increases for a fixed potential height.

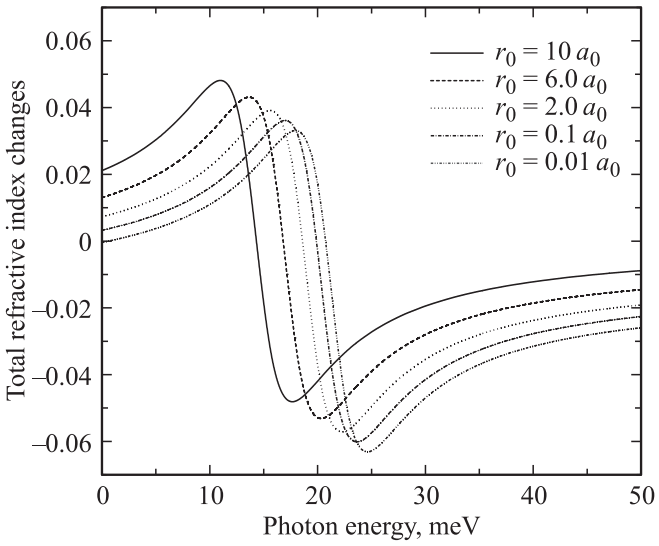

Figure 1. The total refractive index changes as a function of the photon energy for five different antidot size r_0. The parameters used in this figure are and $I = 0.2\,\text{MW/cm}^2$ and $V_0 = 2\,\text{R}_\text{y}$.

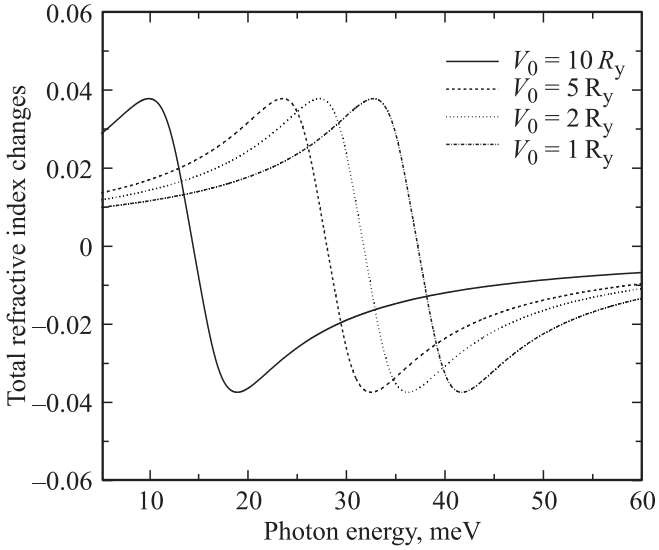

Figure 2. The total refractive index changes as a function of the photon energy for four different potential heights V_0. The parameters used in this figure are $r_0 = 2a_0$ and $I = 0.2\,\text{MW/cm}^2$.

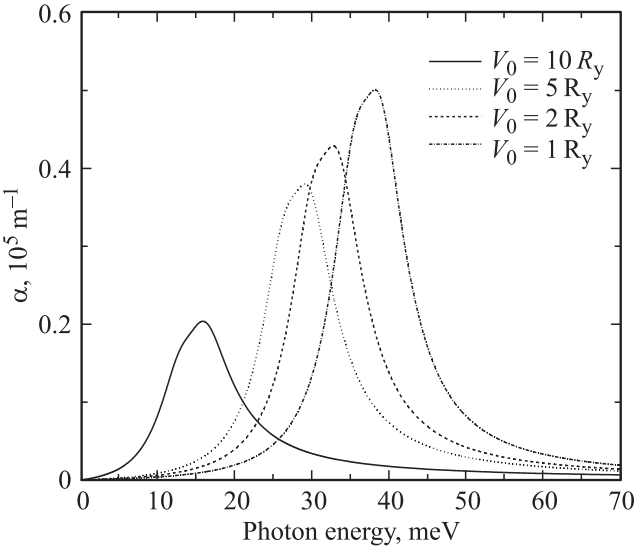

Figure 3. The total absorption coefficient as a function of the photon energy for four different potential heights V_0. The parameters used in this figure are $r_0 = 2a_0$ and $I = 0.2\,\text{MW/cm}^2$.

In Fig. 2, we have plotted the total refractive index changes as a function of the photon energy for four potential height 1, 2, 5, and $10\,\text{R}_\text{y}$ with $I = 0.2\,\text{MW/cm}^2$ and $r_0 = 2a_0$. From this figure, it can be seen that the total refractive index change is related to potential height. As the potential height rises, the total refractive index changes have been reduced in magnitude and also shifted towards higher energies. The main reason for this resonance shift is the increment in energy interval of two different electronic states between which an optical transition occurs.

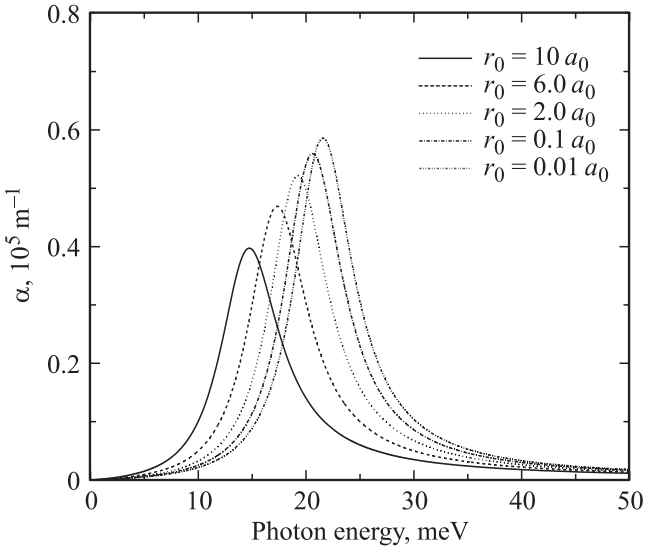

Figure 4. The total absorption coefficient as a function of the photon energy for five different antidot size r_0. The parameters used in this figure are and $I = 0.2\,\mathrm{MW/cm^2}$ and $V_0 = 2\,\mathrm{R_y}$.

In Fig. 3, the variations of total absorption coefficient are plotted as a function of the photon energy with a constant intensity of $I = 0.2\,\mathrm{MW/cm^2}$ for four different potential heights. This figure clearly shows that the peak value of absorption coefficient is directly related to potential height, and, simultaneously, the absorption maximum shifts towards higher energies for increasing potential height.

Fig. 4 shows the total absorption coefficient changes as a function of photon energy with $I = 0.2\,\mathrm{MW/cm^2}$ and $V_0 = 2\,\mathrm{R_y}$ for five different antidot size as 0.01, 0.1, 2, 6, and $10a_0$. Total absorption coefficient change has strongly related to the antidot size, exhibited a red shift as antidot size increases. Moreover, it is obvious form the figure that the magnitude of total absorption coefficient will decrease when the antidot size increases.

5. Conclusion

In this work, we have studied the optical properties of spherical hydrogenic QADs. The antidots are single charged by electrons. We have analytically solved the Schrödinger equation and obtained the energy eigenvalues and wavefunctions. Then, we have calculated the optical absorption coefficients and refractive index changes. We know that the intersubband electronic transitions of the spherical hydrogenic antidots, alter the refractive index we well as the absorption coefficient of the semiconductor medium. In fact the presence of hydrogenic antidot modulates the electronic wave functions and changes the energy levels, thus changing the optical properties of the host medium. The purpose of the present paper is therefore to calculate these changes in the lineal and third order non-linear refractive index as well as absorption coefficient for the medium in the presence of hydrogenic antidot, using the density metrix formalism first introduced in this context in Ref. [17] and used frequently by many authors.

According to the results, we have deduced that i) the total refractive index change increase and also shift towards lower energies as the antidot size increases, ii) when the potential height rises, the total refractive index changes have been reduced in magnitude and also shifted towards higher energies, iii) the peak value of absorption coefficient shifts towards higher energies for increasing potential height, iv) the magnitude of total absorption coefficient will decrease when the antidot size increases.

In summary, it is deduced that antidot size and the potential height play important roles to study the optical properties of spherical hydrogenic QADs.

References

[1] L.C.L.Y. Voon, M. Willatzen. J. Phys. Condens. Matter, **14**, 13 667 (2002).
[2] R. Khordad. J. Luminesc., **134**, 201 (2013).
[3] A. Bagga, S. Ghosh, P. K. Chattopadhyay. Nanotechnology, **16**, 2726 (2005).
[4] K. Karrai, R.J. Warburton. Superlatt. Microstruct., **33**, 311 (2003).
[5] J. Planelles, J.I. Climente, F. Rajadell. Physica E, **33**, 370 (2006).
[6] R. Khordad. J. Opt., **42**, 83 (2013).
[7] J.M. Garsia, G.M. Ribeiro, K. Schmit, T. Ngo, J.L. Feng, A. Lorke, J.P. Kotthaus, P.M. Petroff. Appl. Phys. Lett., **71**, 2014 (1997).
[8] J. Cui, Q. He, X.M. Jiang, Y.L. Fan, X.J. Yang, F. Xue, Z.M. Jiang. Appl. Phys. Lett., **83**, 2907 (2003).
[9] O. Voskoboynikov, C.P. Lee. Physica E, **20**, 278 (2004).
[10] S. Davatolhagh, A.R. Jafari, M.R.K. Vahdani. Superlatt. Microstruct., **51**, 62 (2012).
[11] N. Aquino, E. Castano, E.L. Koo. Cin. J. Phys., **41**, 276 (2003).
[12] C.Y. Hsieh, D.S. Chuu. J. Phys.: Condens. Matter, **12**, 8641 (2000).
[13] V.A. Holovatsky, O.M. Makhanets, O.M. Voitsekhisska. Physica E, **41**, 1522 (2009).
[14] A. Abramowitz, I. Stegun. *Handbook of Mathematical Function with Formulas, Graphs and Mathematical Tables* (Washington DC, US GPO, 1994).
[15] S. Ünlü, I. Karabulut, H. Safak. Physica E, **33**, 319 (2006).
[16] G.H. Wang, Q. Guo, K.X. Guo. Chines. J. Phys., **41**, 296 (2003).
[17] R.W. Boyd. Nonlinear Optics (Academic Press, N.Y., 2003).
[18] D. Ahn, S.L. Chuang. IEEE J. Quant. Electron., **23**, 2196 (1987).
[19] K.J. Kuhn, G.U. Lyengar, S. Yee. J. Appl. Phys., **70**, 5010 (1991).
[20] D.E. Aspnes. Phys. Rev. B, **14**, 5331 (1976).

Редактор Т.А. Полянская